Nuclear Instruments and Methods in Physics Research A 797 (2015) 311–318

Contents lists available at ScienceDirect

Nuclear Instruments and Methods in Physics Research A

journal homepage: www.elsevier.com/locate/nima

Analytical benchmarks for precision particle tracking in electric and magnetic rings

E.M. Metodiev [a,c,d,f], I.M. D'Silva [a], M. Fandaros [a], M. Gaisser [d,f], S. Hacıömeroğlu [a,d,e,f], D. Huang [a], K.L. Huang [a,c], A. Patil [a], R. Prodromou [a], O.A. Semertzidis [a], D. Sharma [a], A.N. Stamatakis [a], Y.F. Orlov [b], Y.K. Semertzidis [a,d,f,*]

[a] Brookhaven National Laboratory, Physics Department, Upton, NY 11973, USA
[b] Department of Physics, Cornell University, Ithaca, NY, USA
[c] Harvard College, Harvard University, Cambridge, MA 02138, USA
[d] Center for Axion and Precision Physics Research, IBS, Daejeon 305-701, Republic of Korea
[e] Istanbul Technical University, Istanbul 34469, Turkey
[f] Department of Physics, KAIST, Daejeon 305-701, Republic of Korea

ARTICLE INFO

Article history:
Received 8 March 2015
Received in revised form
17 May 2015
Accepted 22 June 2015
Available online 30 June 2015

Keywords:
Analytical benchmarking
Precision particle tracking
Electric and magnetic storage rings
Runge–Kutta
Predictor–corrector

ABSTRACT

To determine the accuracy of tracking programs for precision storage ring experiments, analytical estimates of particle and spin dynamics in electric and magnetic rings were developed and compared to the numerical results of a tracking program based on Runge–Kutta/Predictor–Corrector integration. Initial discrepancies in the comparisons indicated the need to improve several of the analytical estimates. In the end, this rather slow program passed all benchmarks, often agreeing with the analytical estimates to the part-per-billion level. Thus, it can in turn be used to benchmark faster tracking programs for accuracy.

© 2015 Elsevier B.V. All rights reserved.

1. Introduction

Analytical estimates for particle dynamics in electric and magnetic rings with and without focusing have been given in a variety of papers and notes. We suggest that these high-precision estimates can serve as benchmarks to test the accuracy of any precision particle tracking program. A program that successfully passes all benchmarks can, in turn, provide a baseline to benchmark faster programs. Thus, it can be a powerful tool for assessing tracking programs for Muon (g-2), Storage Ring EDM and other precision physics experiments requiring high-precision beam and spin dynamics simulation. The program we put to the test in this paper is based on Runge–Kutta/Predictor–Corrector (RKPC) integration, a relatively slow but simple method. It should reproduce the analytical estimates to sub-ppm accuracy on a time scale on the order of hours, in order to be a feasible candidate for benchmarking faster programs. We use the term "focusing" to denote "weak vertical focusing" unless otherwise indicated. Horizontal focusing is defined by the vertical focusing plus the geometry of the ring, always conforming with Maxwell's equations. These benchmarks include the following:

- Pitch correction [1,2] to particle precession frequency in a uniform B-field with and without focusing.
- Vertical oscillations and energy oscillations in a uniform B-field with no focusing, electric focusing, and magnetic focusing.
- Radial and vertical oscillations and energy oscillations in an all-electric ring with and without weak focusing.
- Synchrotron oscillations and momentum capture with a radio frequency cavity (RF) in a uniform B-field.
- An EDM signal and systematic error with an RF Wien Filter in a magnetic ring.

In the analytical estimates that follow, we define γ_0 as the Lorentz factor of the design particle in the ring. The vertical pitch angle θ_y of a particle is defined such that $\theta_y = \beta_z/\beta_\theta$ where $(\beta_\rho, \beta_\theta, \beta_z) = \vec{v}/c$ in cylindrical coordinates. The field focusing index is n, with $n = -(dB/B_0)/(dr/r_0)$ a number with range $0 < n < 1$.

2. Motivation

A tracking program to be used for estimates and investigations in precision experiments must be optimized to be as accurate and

* Corresponding author.

http://dx.doi.org/10.1016/j.nima.2015.06.032
0168-9002/© 2015 Elsevier B.V. All rights reserved.

fast as possible. This calls for a well-tested and robust procedure to benchmark the accuracy of tracking programs in situations relevant to the experiments. Precision experiments such as the Muon (g-2) and Storage Ring Electric Dipole Moment (EDM) experiment [3–5] require measurements of sub-part per million (ppm) accuracy. In the case of a proton or deuteron Storage Ring EDM experiment, a tracking program of extraordinary precision is required to estimate the spin coherence time of the particle distribution and various lattice parameters, as well as to estimate the values of systematic errors associated with the experiment. Many commonly used beam and spin dynamics programs ignore, or erroneously account for, second and higher-order effects. Tracking in an electric storage ring poses the additional challenge of conforming with total-energy conservation while accounting for higher-order effects.

Numerical integration with a sufficiently small step size allowed to run for a sufficiently long time may reproduce the analytical results with high accuracy. Moreover, comparison of analytical estimates with precision tracking results can identify discrepancies and indicate the need to improve the estimates. (In this way, it was determined that the total correction due to vertical particle oscillations, the so-called pitch effect, can be significantly reduced [6].)

We benchmarked a program based on Runge–Kutta/Predictor–Corrector method [7] against the developed analytical estimates.

3. Precision tracking

For a particle of mass m and charge e, there are two differential equations that govern particle and spin dynamics. For particle velocity $\vec{\beta}$ and rest spin $\vec{s}$ in external fields, the equations are [8]

$$\frac{d\vec{\beta}}{dt}=\frac{e}{m\gamma c}\left[\vec{E}+c\vec{\beta}\times\vec{B}-\vec{\beta}(\vec{\beta}\cdot\vec{E})\right], \tag{1}$$

and the T-BMT equation, with an anomalous magnetic moment a of the particle:

$$\frac{d\vec{s}}{dt}=\frac{e}{m}\vec{s}\times\left[\left(a+\frac{1}{\gamma}\right)\vec{B}-\frac{a\gamma}{\gamma+1}\vec{\beta}(\vec{\beta}\cdot\vec{B})-\left(a+\frac{1}{\gamma+1}\right)\frac{\vec{\beta}\times\vec{E}}{c}\right]. \tag{2}$$

The RKPC integration was used with a step size of 1–10 ps to numerically solve the two differential equations with the corresponding initial conditions.

4. Magnetic ring

A magnetic ring consists of a uniform magnetic field $\vec{B}$, taken to be in the vertical direction. The correction C to the precession frequency due to a vertical pitch is defined by $\omega_m=\omega_a(1-C)$, where ω_a is the $(g-2)$ correct frequency [9] for a particle with anomalous magnetic moment a, and ω_m is the measured frequency. The predicted correction is [2]

$$C=\frac{1}{4}\theta_0^2\left\{1-(\omega_a^2+2a\gamma^2\omega_p^2)/\gamma^2(\omega_a^2-\omega_p^2)\right\}. \tag{3}$$

with $\omega_p=2\pi f_p$, where f_p is the vertical (pitch) oscillation frequency.

4.1. No focusing

When there is no focusing or when $\omega_p \ll \omega_a$, the correction from Eq. (3) becomes

$$C=\frac{1}{4}\beta^2\theta_0^2, \tag{4}$$

where for linear oscillations, $\langle\theta_y^2\rangle=(1/2)\theta_0^2$, where θ_0 is the maximum pitch angle of the particle trajectory.

For a particle with $\beta=0.972$ and a constant 1.0 mrad vertical pitch as shown in Fig. 1, the simulated correction to the $(g-2)$ precession frequency of 0.2361 ppm is in very good agreement with the analytically predicted value of 0.2363 ppm using Eq. 4.

Checking over several values of θ_y confirms that the analytic expression and the pitch correction in the tracking simulation agree for small θ_y, as expected.

4.2. Weak magnetic focusing

When there is magnetic focusing and when $\omega_p \gg \omega_a$, the correction from Eq. (3) becomes

$$C=\frac{1}{4}\theta_0^2(1+2a). \tag{5}$$

The analytical estimate [10] for the average particle radial deviation from the ideal orbit with radius r_0, with weak magnetic focusing index n, takes the form

$$\left\langle\frac{\Delta r}{r_0}\right\rangle=\alpha_p\left\langle\frac{\Delta p}{p_0}\right\rangle=-\frac{1}{1-n}\left\langle\theta_y^2\right\rangle, \tag{6}$$

for a vertical pitch frequency significantly greater than the $(g-2)$ precession frequency of the particle, where α_p is the momentum compaction factor.

Eq. (6) predicts an average radial deviation $\langle\Delta r/r_0\rangle$ of -5×10^{-7} using $\theta_0=1$ mrad and a field index $n=0.01$, consistent with the tracking results shown in Fig. 2 to sub-part per billion (ppb) level. The dependence of $<\Delta r/r_0>$ on the field index is shown to hold over a range of n values in Fig. 3.

In a continuous storage ring with weak focusing, field strength B_0, and ring radius r_0, the vertical and horizontal magnetic field components around the ideal trajectory can be expressed to second-order in the vertical position y as

$$B_x(x,y)=-n\frac{B_0}{r_0}y \tag{7}$$

$$B_y(x,y)=B_0-n\frac{B_0}{r_0}x+n\frac{B_0}{r_0}\frac{y^2}{2r_0}, \tag{8}$$

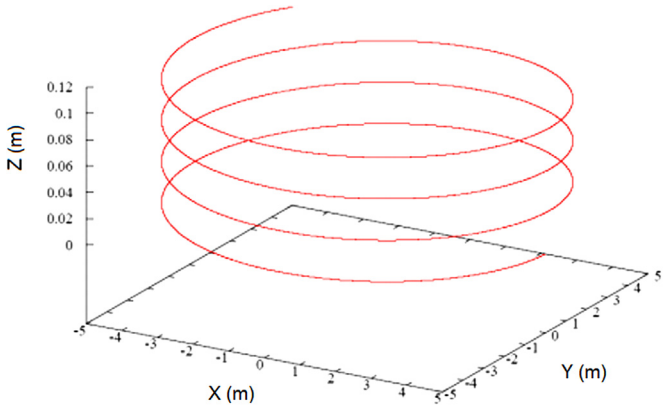

Fig. 1. The particle path in Cartesian coordinates in a uniform B-field with pitch angle $\theta_y=1.0$ mrad, for a ring with a 5 m radius.

where the nonlinearity arises from the application of Maxwell's equations in cylindrical coordinates. The horizontal and vertical tunes are given by $\nu_x = \sqrt{1-n}$ and $\nu_y = \sqrt{n}$ respectively.

We make use of the relations [10] from Eq. (6):

$$\frac{<x>}{r_0} = -\alpha_p \frac{\theta_0^2}{2} = -\frac{1}{1-n}\frac{\theta_0^2}{2}, \tag{9}$$

and $\theta_0 = y_0/(r_0/\sqrt{n})$, where y_0 is the maximum vertical excursion. From this we see that

$$C_B = \left\langle \frac{B_y}{B_0} - 1 \right\rangle = -\frac{n}{r_0}<x> + n\frac{y_0^2}{4r_0^2} = \frac{n}{1-n}\frac{\theta_0^2}{2} + \frac{\theta_0^2}{4}. \tag{10}$$

By considering the time-averaged relative B-field change, calling C_B the modification due to the different B-field encountered by the particle, we find that the correction $C^* = C - C_B$ to the $(g-2)$ precession frequency in a magnetic storage ring with weak focusing, i.e. $\omega_m = \omega_a(1-C^*)$, is given by the expression:

$$C^* = \left(a - \frac{n}{1-n}\right)\frac{\theta_0^2}{2}. \tag{11}$$

Here we see that several terms of the inhomogeneous B-field correction and the correction in Eq. 5 cancel, leaving a small correction. The necessity of including the second-order inhomogeneous magnetic field contributions was overlooked by previous authors. Thus, investigating the precision of the tracking program identified an oversight and led back to improvement of the analytical estimate.

This correction holds for a vertical pitch frequency much greater than the $(g-2)$ precession frequency of the particle, which for a weak focusing ring means $\sqrt{n} \gg a\gamma$. Eq. (11) implies that the pitch effect can, in principle, be made to vanish for $n = a/(1+a)$, but the condition $\sqrt{n} \gg a\gamma$ makes it rather difficult to achieve. To test the tracking program we introduced a particle with 10 times the muon mass, with same a value as the muon, stored in a ring radius of 7.112 m. The program indeed showed that the pitch correction vanishes with an uncertainty at the part per billion (ppb) level when $n = a/(1+a)$ was used.

For realistic muon parameters, the observed $(g-2)$ frequency is off from its correct value by $+0.109$ ppm, for a vertical maximum pitch angle $\theta_0 = 1$ mrad, and $n = 0.18$, consistent with the offset shown in Fig. 4 to sub-ppb level.

A resonance of the pitch effect correction occurs when the vertical pitch frequency ω_p is equal to the $(g-2)$ precession of the stored particles ω_a. The correction C approaches Eq. (4) for $\omega_p \ll \omega_a$ and Eq. 5 for $\omega_p \gg \omega_a$. The full range of pitch corrections C over a range of index values is shown in Fig. 5. When all the fields are taken properly into account, as shown above, the tracking results reproduce the same curve to sub-ppb level for $\Delta\omega_a/\omega_a$.

A comparison of the frequency shift predicted by Eq. (11) and the results from tracking is given in Table 1. The analytical estimates of the pitch correction and the tracking results are in very good agreement, better than ppb level. This level of precision is adequate for the Muon $g-2$ experiments currently underway [6,11], both aiming for better than 0.1 ppm total systematic error.

4.3. Weak electric focusing

In the case of electric focusing in a uniform magnetic ring, the expected precession frequency correction due to the pitch effect is [2]

$$C = \frac{1}{4}\theta_0^2\left\{\beta^2 - (a^2\beta^4\gamma^2\omega_p^2)/(\omega_a^2 - \omega_p^2)\right\}. \tag{12}$$

and

$$C = \frac{1}{4}\theta_0^2\beta^2(1+a), \tag{13}$$

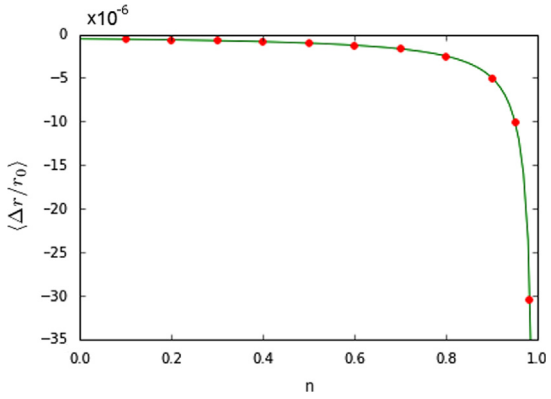

Fig. 3. The average $\langle \Delta r/r_0 \rangle$ versus the field focusing index n. The solid line represents the predicted values while the points are the results of tracking. The simulation used a maximum pitch angle of $\theta_0 = 1.0$ mrad.

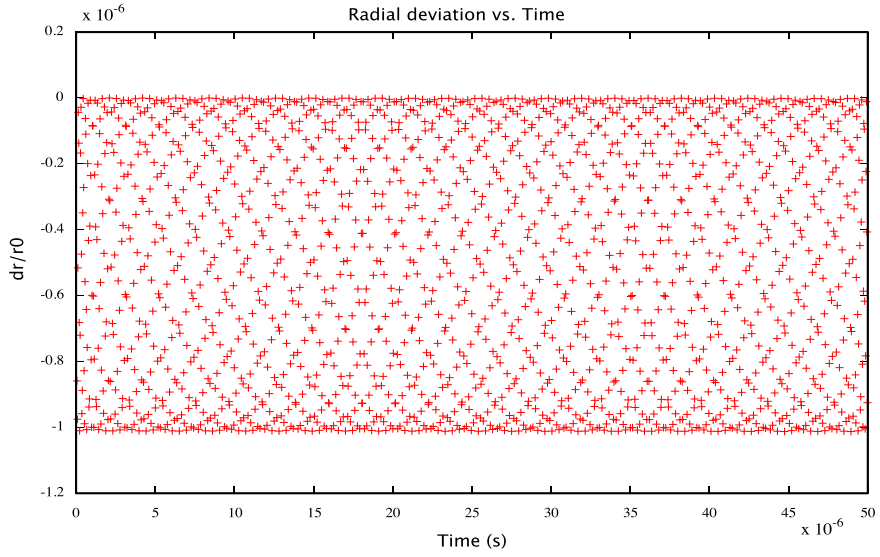

Fig. 2. The particle deviation from the ideal radial position over time, modulo 50 μs. The simulations used a maximum pitch angle of $\theta_0 = 1$ mrad and magnetic focusing with field index $n = 0.01$.

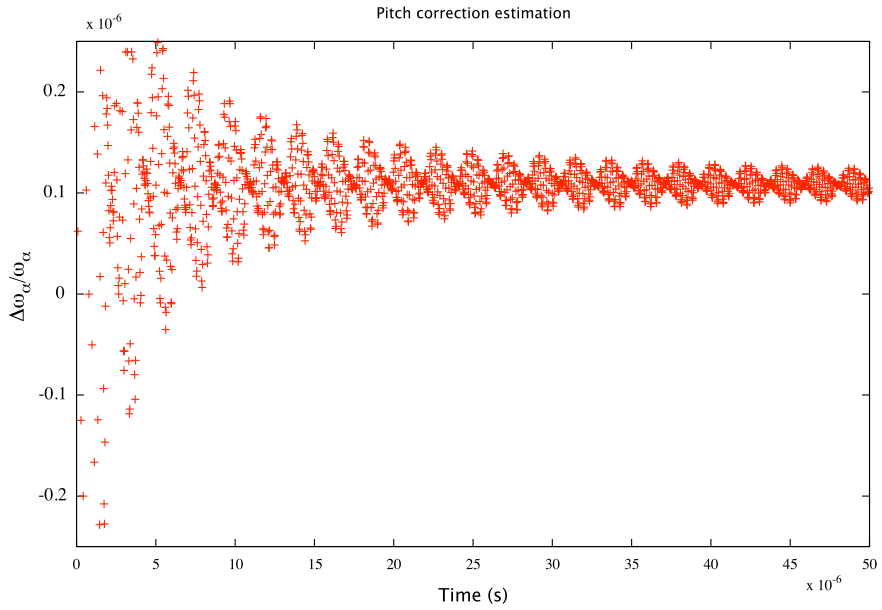

Fig. 4. The pitch correction to the $(g-2)$ frequency with angle $\theta_0 = 1.0$ mrad, $\gamma = 29.3$, and $n = 0.18$, is 0.109 ppm, consistent with Eq. (11) to sub-ppb level.

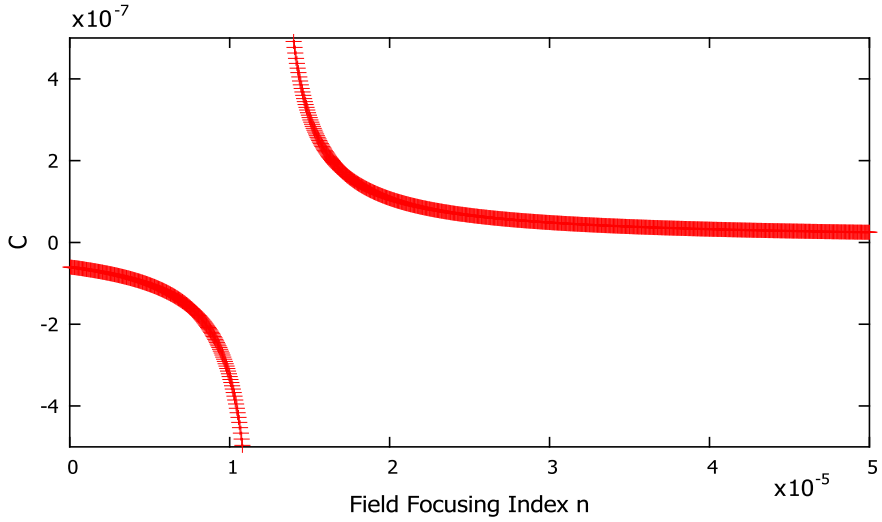

Fig. 5. Parameter C from Eq. (3) for the pitch correction to the $(g-2)$ frequency over a range of n values using $\theta_y = 1.5$ mrad and $\beta = 0.94$. A resonance occurs when $\omega_p = \omega_a$, at $n \approx 1.25 \times 10^{-5}$, as expected.

Table 1
Comparison of the frequency shift estimated using Eq. (11) and the tracking results. The tracking results assume a muon with $\gamma = 29.3$, stored in a magnetic ring with magnetic focusing and a radius $r_0 = 7.112$ m. The vertical angle used is $\theta_y = 0.5$ mrad. The observed $g-2$ frequency is shifted higher by the small factors given below depending on the n-value used.

n	Estimation (ppb)	Tracking (ppb)
0.01	1.1	1.0
0.02	2.4	2.4
0.03	3.7	3.6
0.05	6.4	6.4
0.08	10.7	10.8
0.10	13.7	13.7
0.137	19.7	19.9
0.237	38.7	38.8

for $\omega_p \gg \omega_a$ and for the particle at the magic momentum [4,5] such that an electric field does not affect the $(g-2)$ precession.

For a maximum vertical pitch of $\theta_0 = 0.5$ mrad, the analytically estimated pitch correction of 0.0624 ppm for magic momentum muons is very close to the result from tracking, shown in Fig. 6, consistent to sub-ppb level.

Since the results from tracking match the predicted value to this level of accuracy, we conclude that the analytical estimates and the RKPC integration method have passed the magnetic ring tracking benchmarks.

4.4. Radio frequency cavity

The synchrotron oscillation frequency f_s of a particle in a uniform B-field with an RF is

$$f_s = Q_s f_c, \tag{14}$$

where f_c is the cyclotron frequency and Q_s is the synchrotron tune, which satisfies

$$Q_s^2 = \frac{eV_0 \eta_c h}{2\pi c p_0 \beta^2}. \tag{15}$$

In the expression above, e is the elementary charge, V_0 is the voltage of the RF cavity, h is the harmonic of the RF cavity used,

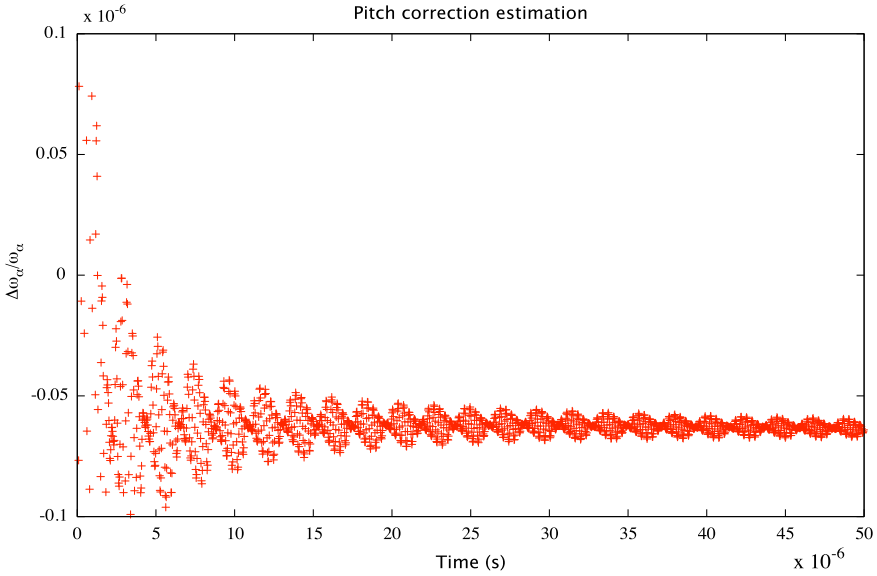

Fig. 6. The relative difference between the ideal $(g-2)$ and the actual precession of a particle with a maximum pitch angle of $\theta_0 = 0.5$ mrad, estimated from tracking using electric focusing in a magnetic ring. To obtain the correct $g-2$ frequency, the correction $0.25 \times \theta_0^2$ needs to be added to the observed frequency. Again, the tracking results are consistent with the predictions to sub-ppb level.

and p_0 is the ideal momentum. The value of η_c, the so-called slip factor, is determined from the expression:

$$\eta_c = \alpha_p - \frac{1}{\gamma_0^2} = \frac{1}{1-n} - \frac{1}{\gamma_0^2}. \tag{16}$$

Using a particle with charge e, $p_0 = 3.094$ GeV/c, and $\gamma_0 = 29.3$, and using a 20 cm RF cavity with $V_0 = 100$ kV and harmonic $h=1$, the predicted synchrotron frequency with $n=0.18$ is $f_s = 16.8$ kHz and with no vertical focusing it is $f_s = 15.2$ kHz. Comparing these calculations with the results of tracking in Fig. 7 shows close agreement between the tracking simulation and the estimation, verified at the 0.1% level.

The maximum momentum capture range of the RF cavity [12] is given by the expression:

$$\left(\frac{\Delta p}{p_0}\right)_{\max} = \sqrt{\left|\frac{2eV_0}{\pi h \eta_c \beta c p_0}\right|}, \tag{17}$$

around the ideal particle with momentum p_0.

Using the above RF parameters and particle values, the maximum stored momentum is estimated from Eq. (17) to be $(\Delta p/p_0)_{\max} = 0.00454$ with no vertical focusing. The momentum capture range of the configuration illustrated by the RF phase diagram in Fig. 8 is consistent with the estimated value.

Thus, in the case of a magnetic ring we see agreement to the desired accuracy between the results of RKPC integration and the analytical estimates of both maximum stored momentum and synchrotron frequency.

5. Electrostatic ring

In cylindrical coordinates, the electric field with an index m power law dependence on radius at $y=0$ is

$$\vec{E}(r,0) = E_0 \frac{r_0^{1+m}}{r^{1+m}} \hat{r}, \tag{18}$$

where $\hat{y}$ is the vertical direction and $\hat{r}$ is in the radial direction.

In a uniform all-electric ring, we have found that the $y \to -y$ and rotational symmetries allow the radial and vertical electric

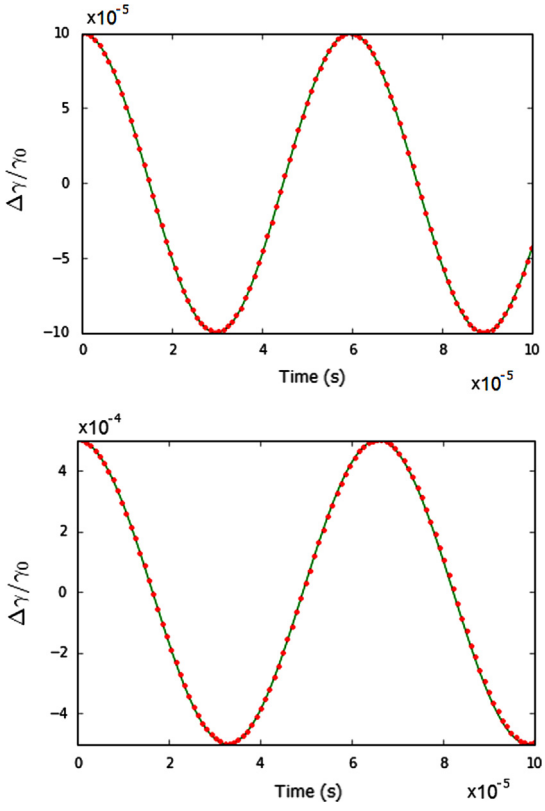

Fig. 7. The synchrotron oscillations of a particle in a uniform B-field with an RF with (top) $n=0.18$ and (bottom) no vertical focusing. The solid line represents the estimated oscillations; the points are the results of tracking.

field components to be found exactly:

$$E_y(r,y) = E_0 \frac{r_0^{1+m}}{r^{1+m}} \frac{my}{r} {}_2F_1\left(1+\frac{m}{2}, 1+\frac{m}{2}; \frac{3}{2}; -\frac{y^2}{r^2}\right) \tag{19}$$

$$E_r(r,y) = E_0 \frac{r_0^{1+m}}{r^{1+m}} {}_2F_1\left(1+\frac{m}{2}, \frac{m}{2}; \frac{1}{2}; -\frac{y^2}{r^2}\right), \tag{20}$$

for all $m > 0$, where ${}_2F_1$ is the ordinary hypergeometric function.

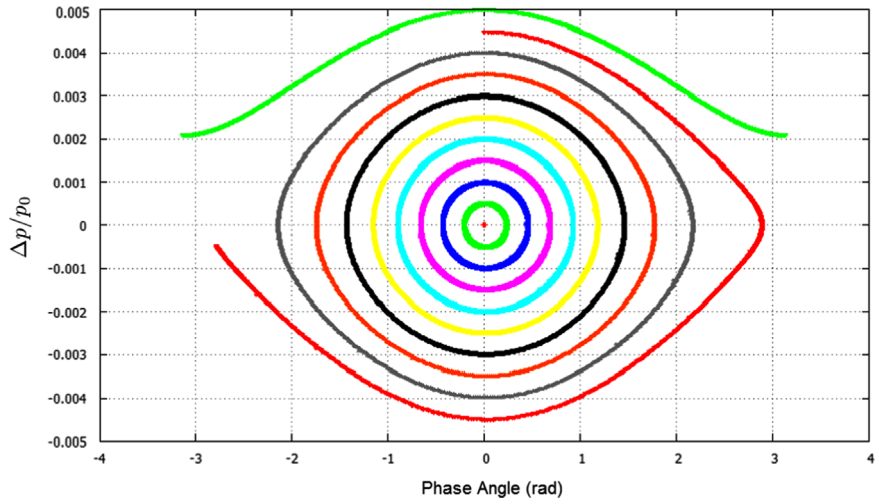

Fig. 8. A phase diagram of particle momenta in a uniform B-field with an RF and no vertical focusing. The closed energy oscillations around the synchronous particle define the momentum capture range of the RF. The unstored particle is close to the boundary of the storage region.

The field index is $n=m+1$, and $m=0$ corresponds to cylindrical plates with no vertical focusing, $m=1$ corresponds to spherical plates, and so on. The focusing m value depends on the choice of electrode profile.

For $m=0$, the electric field is that of a uniform cylindrical capacitor. The fields were taken to fifth-order in y/r when implemented in the tracking program. The expansion to second-order is shown below:

$$E_r(r,y)=E_0\frac{r_0^n}{r^n}\left[1-\frac{1}{2}(n^2-1)\frac{y^2}{r^2}+\mathcal{O}\left(\frac{y^4}{r^4}\right)\right] \tag{21}$$

$$E_y(r,y)=E_0\frac{r_0^n}{r^n}\left[(n-1)\frac{y}{r}+\mathcal{O}\left(\frac{y^3}{r^3}\right)\right]. \tag{22}$$

The contributions of the higher-order electric field terms were found to be negligible for tracking. The second-order term is significant for the analytical estimates. The fields given in Eqs. (19) and (20) describe the field configuration considered for an electric ring.

In an all-electric ring, the kinetic energy changes with the radial position, which provides additional horizontal focusing. The horizontal and vertical tunes [13,14] are given by $\nu_x=\sqrt{1-m+1/\gamma^2}$ and $\nu_y=\sqrt{m}$ respectively, in an electric ring with weak focusing.

5.1. No focusing, including an RF cavity

With no focusing in the ring, we have $n=1$ and thus $m=0$, corresponding to concentric cylindrical plates. We also include an RF-cavity, which fixes the particle revolution frequency. Y. Orlov [15,16] and I. Koop [17] solved the orbital motion for an electrostatic field with no focusing. In this case, the estimates for the average values of $\Delta\gamma/\gamma_0$ and $\Delta r/r_0$ take the following form:

$$\left\langle\frac{\Delta\gamma}{\gamma_0}\right\rangle=\langle\theta_y^2\rangle\frac{\gamma_0^2-1}{\gamma_0^2+1}, \tag{23}$$

$$\left\langle\frac{\Delta r}{r_0}\right\rangle=-\frac{\langle\theta_y^2\rangle}{2}\frac{\gamma_0^2-1}{\gamma_0^2+1}. \tag{24}$$

Note that these values depend only on the particle's ideal Lorentz factor γ_0 and the pitch angle, not on the ring radius, plate spacing, or electric field strength.

The precision tracking results for the two parameters and the predicted values of Eqs. (23) and (24) are shown in Fig. 9. We see close agreement between the expected value and the values calculated through tracking. Incidentally, we found from tracking that without including an RF-cavity, $\left\langle\frac{\Delta r}{r_0}\right\rangle$ from Eq. (24) becomes

$$\left\langle\frac{\Delta r}{r_0}\right\rangle=-\langle\theta_y^2\rangle\frac{\gamma_0^2}{\gamma_0^2+1}, \tag{25}$$

whereas Eq. (23) remains the same.

5.2. Weak electric focusing, including an RF cavity

With weak focusing such that $0<m\ll 1$, the parameters analytically estimated by Y. Orlov [15,16] are given by Eqs. (26) and (27) below:

$$\left\langle\frac{\Delta\gamma}{\gamma_0}\right\rangle=0, \tag{26}$$

$$\left\langle\frac{\Delta r}{r_0}\right\rangle=-\frac{1}{2}\langle\theta_y^2\rangle, \tag{27}$$

which hold for times much larger than the period of vertical oscillations. Note that these values depend only on the pitch angle and not on the ring geometry, ideal γ_0 or field focusing index.

There is an apparent gap between Eqs. (23) and (24), and Eqs. (26) and (27) in the limit as $m\to 0$. The transition between focusing and no focusing can exist since the latter formulas hold only for averages over times much larger than the period of vertical oscillations [16].

Figs. 10 and 11, which present tracking results and analytical estimates for $<\Delta\gamma/\gamma_0>$ and $<\Delta r/r_0>$, respectively, show a close match between them. There is a vertical spread of less than one part per billion for $<\Delta\gamma/\gamma_0>$ and less than 0.1 ppm for $<\Delta r/r_0>$, which we assign as the error of the RKPC method.

That the tracking results match the predicted $<\Delta\gamma/\gamma_0>$ and $<\Delta r/r_0>$ values to sub-ppm accuracy, as shown in Figs. 9–11, again shows that the RKPC method passes the electric field benchmark. From these comparisons, we see again that the analytical estimates and the Runge–Kutta/Predictor–Corrector method pass the electric field benchmarks.

6. Radio frequency Wien filter

A radio frequency Wien filter (WF) is a velocity-dependent charged particle filtering device. A WF can be used in a storage ring to measure a particle's electric dipole moment (EDM). The

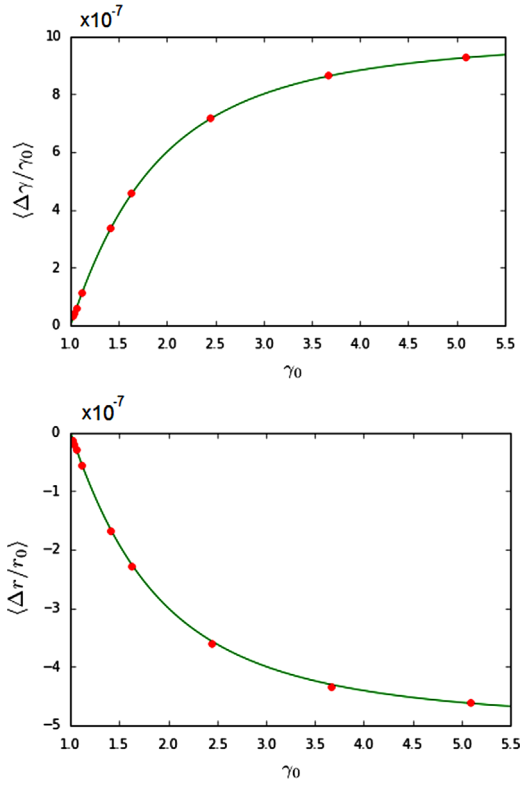

Fig. 9. The average $\langle \Delta\gamma/\gamma_0 \rangle$ (on top) and average $\langle \Delta r/r_0 \rangle$ (on bottom) versus the ideal γ_0 of the proton. The solid lines represent the predicted values; the points are the results of tracking. The simulation used a pitch angle of $\theta_y = 1.0$ mrad, an RF-cavity and no vertical focusing.

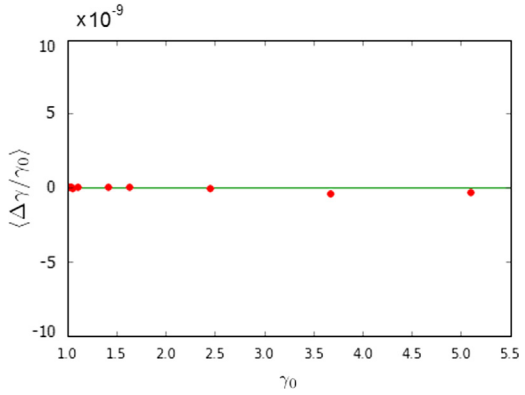

Fig. 10. The average $\langle \Delta\gamma/\gamma_0 \rangle$ versus the ideal γ_0 of the proton over a variety of focusing n values. The solid line represents the predicted values; the points are the results of tracking. The simulation used $\theta_0 = 1.0$ mrad, an RF-cavity and vertical focusing.

analytical estimates [18] of the EDM signal and systematic error for a particle of charge e, mass m, and anomalous magnetic moment a in electric and magnetic fields are

$$\left(\frac{ds_V}{dt}\right)_{edm} = \eta\frac{eb_V}{4mc}\frac{(1+a)}{\gamma^2}s_{L0}\frac{e(-E_R+\beta B_V)}{mc\omega_{a,0}}, \tag{28}$$

$$\left(\frac{ds_V}{dt}\right)_{sys} = \frac{eb_{R0}}{2mc}\frac{(1+a)}{\gamma^2}s_{L0}, \tag{29}$$

where s_{L0} is the peak longitudinal spin magnitude, E_R is the radial electric field strength, and B_V is the vertical magnetic field strength. The EDM is proportional to η, with η playing the same

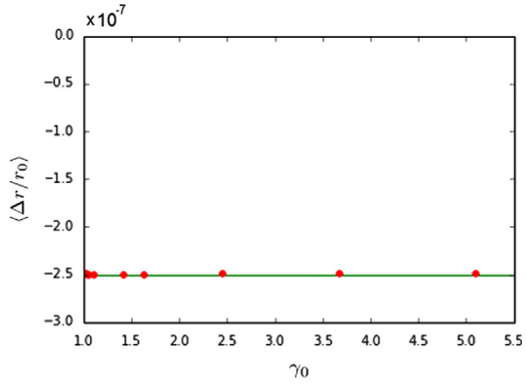

Fig. 11. The average $\langle \Delta r/r_0 \rangle$ versus the ideal γ_0 of the proton over a variety of focusing n values. The solid line represents the predicted values; the points are the results of tracking. The simulation used $\theta_0 = 1.0$ mrad, an RF-cavity and vertical focusing.

Table 2
Radio frequency Wien filter: comparison between analytical estimates and tracking results for the deuteron case, in rad/s. Momentum p is in GeV/c. The EDM value is assumed to be $10^{-18} e \cdot$ cm, while for the (systematic) error, the misalignment angle is assumed to be 0.1 mrad.

p	EDM tracking	EDM analytic	Error analytic	Error tracking
0.7	−1.00	−1.00	0.41	0.41
1.4	−0.74	−0.73	0.175	0.17
2.1	−0.50	−0.51	0.096	0.097
2.8	−0.36	−0.35	0.063	0.06

Table 3
Radio frequency Wien filter: comparison between analytical estimates and tracking results for the proton case, in rad/s. Momentum p is in GeV/c. The EDM value is assumed to be $10^{-18} e \cdot$ cm, while for the (systematic) error the misalignment angle is assumed to be 0.1 mrad.

p	EDM tracking	EDM analytic	Error analytic	Error tracking
0.7	0.357	0.357	1.135	1.137
1.4	0.174	0.172	0.393	0.396
2.1	0.0934	0.093	0.192	0.195
2.8	0.0566	0.0563	0.1135	0.1135

role for the EDM as the g-factor plays for the magnetic dipole moment. The radio frequency WF ideally produces a vertical magnetic field at the $g-2$ frequency $b_V = b_{V0}\cos\omega_{a0}t$ and a radial electric field $e_R = e_{R0}\cos\omega_{a0}t$ with the condition [18] $e_{R0} = \beta b_{V0}$. However, if the WF is misaligned by an angle θ with respect to the vertical, then a radial B-field will also be present $b_R = b_{R0}\cos\omega_{a0}t$, with $b_{R0} = b_{V0}\sin\theta$ inducing a systematic error given by Eq. (29).

A comparison between the analytical estimates and the tracking results for the deuteron case and the proton case are given in Tables 2 and 3, respectively.

The Wien Filter provides another benchmark for testing the accuracy of the analytical estimates and the RKPC tracking method. We again see very good agreement between the analytically predicted values and those calculated by tracking.

7. Conclusion

Our array of analytical estimates has been shown to be a powerful tool for benchmarking programs which simulate particle motion and

spin dynamics in electric and magnetic rings, with and without focusing, as well as RF cavities and Wien filters. The tested program, based on Runge–Kutta/Predictor–Corrector integration, passed all benchmarks, often agreeing with the analytical estimations to the part-per-billion level. Therefore, this accurate (albeit slow) program can in turn be used to benchmark faster tracking programs whose accuracy is unknown, as well as confirm the perceived accuracy of programs like in [19,20]. Moreover, the benchmarking process can also, in principle, result in improved analytical estimates, as in the case of the pitch effect here.

Acknowledgments

We would like to thank the Department of Energy and Brookhaven National Laboratory for their continued support of the High School and Supplemental Undergraduate Research Programs. We especially thank the Storage Ring EDM collaboration. DOE partially supported this project under BNL Contract No. DE-SC0012704. IBS-Korea partially supported this project under system code IBS-R017-D1-2014-a00. We also thank Sidney Orlov, who has greatly improved the clarity of this paper.

References

[1] J.H. Field, G. Fiorentini, Il Nuovo Cimento 21A (1974) 297.
[2] F.J.M. Farley, Physics Letters 42B (1972) 66.
[3] G.W. Bennett, et al., Physical Review D 73.7 (2006) 072003.
[4] V. Anastassopoulos et al., A Proposal to Measure the Proton Electric Dipole Moment with 10^{-29} e·cm Sensitivity, Available at http://www.bnl.gov/edm, Storage Ring EDM Collaboration, 2011.
[5] V. Anastassopoulos, et al., A Storage Ring Experiment to Detect a Proton Electric Dipole Moment, Storage Ring EDM Collaboration, 2011. arXiv:physics.acc-ph/1502.04317.
[6] T. Mibe, Nuclear Physics B: Proceedings Supplements 218.1 (2011) 242.
[7] R.W. Hamming, Journal of the ACM (JACM) 6 (1959) 37.
[8] J.D. Jackson, Classical Electrodynamics, third ed., Wiley, New York, 1998.
[9] G.W. Bennett, et al., Physical Review D 73 (2006) 072003.
[10] E.D. Courant, H.S. Snyder, Annals of Physics 3 (1958) 1.
[11] J. Grange, et al., Muon (g–2) Technical Design Report, Fermilab E 989, 2015. arXiv:1501.06858.
[12] M. Conte, W.W. MacKay, An Introduction to the Physics of Particle Accelerators, World Scientific, Singapore, 1991.
[13] L.J. Laslett, ERAN-30 Note (1969) included in Selected Works of L. Jackson Laslett, LBL PUB616, 1987, section 3, p. 13.
[14] S.R. Mane, Nuclear Instruments and Methods in Physics Research Section A 596 (2008) 288.
[15] Y.F. Orlov, Spin Coherence Time Analytical estimates. EDM Searches at Storage Rings, ECT Trento. 1–5 October, 2012.
[16] Y.F. Orlov, Confirmation of some formulas related to spin coherence time, and references therein, April 2015. arxiv.org/abs/1504.07304.
[17] Appendix A in S.R. Mane, Nuclear Instruments and Methods in Physics Research A 767 (2014): 252–261.
[18] W.M. Morse, Y.F. Orlov, Y.K. Semertzidis, Physical Review Special Topics—Accelerators and Beams 16 (2013) 114001.
[19] S. Hacıömeroğlu, Y.K. Semertzidis, Nuclear Instruments and Methods in Physics Research Section A 743 (2014) 96.
[20] S.R. Mane, Nuclear Instruments and Methods in Physics Research A 769 (2015) 26.